JOURNAL OF MATERIALS SCIENCE **38** (2003) 2913–2923

Statistical analysis of the failure stresses of ceramic fibres: Dependence of the Weibull parameters on the gauge length, diameter variation and fluctuation of defect density

M.-H. BERGER
Ecole Nationale Supérieure des Mines de Paris, Centre des Matériaux, BP87, 91003 Evry Cedex, France
E-mail: marie-helene.berger@ensmp.fr

D. JEULIN
Ecole Nationale Supérieure des Mines de Paris, Centre de Morphologie Mathématique, 35 rue Saint-Honoré, 77305 Fontainebleau, France. Now at ISTASE, Université Jean Monnet, 23 rue du Docteur Paul Michelon, 42023 Saint-Etienne Cedex 2, France

The strength distribution of ceramic fibres is commonly described using a two-parameter Weibull distribution function. This study shows that the determination of these parameters from around 30 tensile tests obtained at one single gauge length (L_0) does not allow the strength distribution at other gauge lengths to be correctly predicted. The reliability in the Weibull parameter determination is lowered by variations in fibre diameter (D) and the insufficient number of fibres tested. An effective failure stress $\sigma_E = \sigma \cdot (\pi D \cdot L_0)^{1/m}$ is first introduced to take into account fibre diameter variations and to extract the two Weibull parameters from the 180 tests obtained at 6 gauge lengths. It is then shown that the linear size effect, which is expected from the standard Weibull model, is not appropriate to fit correctly this experimental strength distribution. The length dependence follows a power law (L_0^{β}) leading to an effective failure stress $\sigma_E = \sigma \cdot (\pi D \cdot L_0^{\beta})^{1/m}$. Diameter variations along the gauge length cannot be responsible for this non linear variation with the length, which is attributed to a large scale fluctuation of the density of defects. The value of β can bring valuable information about fluctuations in the fibre processing conditions.

1. Introduction

Small diameter ceramic fibres are used as reinforcements for brittle matrix composites the behaviour of which depends strongly on the properties of the fibres. In order to design structures in such composite materials it is necessary to be able to quantify the strengths of the fibres. However the failure stresses of ceramic fibres show considerable scatter so that a statistical approach is necessary to predict the failure stresses of the fibres used in structures.

Testing bundles of fibres could allow the stress distribution of the fibres of the bundle to be obtained, [1, 2]. However it may introduce some ambiguities concerning the number of fibres which are effectively loaded. The load distribution among the fibres in the case when these fibres are not perfectly aligned and identically stretched at the beginning of the tensile test is not known precisely. Tensile tests conducted with single fibres give a straighter determination of the failure stress distribution of the fibres inside the bundle, but, in order to obtain the data necessary for a statistical analysis, many test results have to be obtained.

The distribution of the failure stresses of brittle ceramic fibres is most often analysed using the Weibull statistical model. This model is based on the failure of a chain in which the weakest link controls rupture and seems to be well adapted to describe a set of tensile test results carried out at one gauge length. The analysis of a wide range of ceramic fibres (SiC based fibres and oxide fibres) at different gauge lengths has however permitted to draw limitation that a blind utilisation of the Weibull model could give. The aim of this paper is to point out common restrictions or remarks that arise from this analysis and to propose another formulation of the model. This work will be illustrated by the study of the tensile properties of the mullite-alumina Nextel 720 fibre [3] produced by 3M [4].

2. Specimen preparation

Traditionally a number, often around thirty, of individual fibres of identical lengths are tested in tension. The fibres have to be carefully extracted from the bundle. This is achieved by immersing a length of the bundle slightly longer than the gauge length inside absolute alcohol in a rectangular and flat container and separating it gently into around five meshes. One single fibre extremity is then held between gloved fingers and carefully pulled out from the mesh. The fibre is then placed on a cardboard frame, aligned on a straight line and fixed with epoxy glue. The distance between the two glue points defines the gauge length, which is marked by two holes on the cardboard. Two other holes allow the cardboard to be fixed to the grip assembly, and other apertures are made every 50 mm for the fibre diameter to be measured optically using an image shearing eyepiece[1] or a laser scan micrometer[2]. The prepared sample is fixed on the tensile machine [5] and the central part of the cardboard is removed by cutting lateral slots from the holes which define the gauge length. Fracture morphologies are observed in a SEM, to determine whether the defect which initiated fracture is located on the fibre surface or inside the fibre.

3. The classical use of the Weibull statistical model

The survival probability P_S of a fibre of diameter D and length L_0 under a stress σ, can be first modelled using a unimodal Weibull distribution with a volume or a surface dependence, according to the defect location:

$$P_S(\sigma_R \geq \sigma) = \exp(-\theta_S \cdot \sigma^m \cdot S) \quad (1)$$

if defects are located on the fibre surface, and

$$P_S(\sigma_R \geq \sigma) = \exp(-\theta_V \cdot \sigma^m \cdot V) \quad (2)$$

if defects are located in the fibre volume, where σ_R is the failure stress of the fibre, m is the Weibull modulus, which characterises the width of the failure stress distribution, that is the dispersion of the size of the defects in the fibre, $\theta_S\sigma^m$ and $\theta_V\sigma^m$ are the intensity (average number per unit length) of defects associated to a failure stress lower than σ for defects located on the external fibre surface and in the fibre volume respectively. S is the external surface of the fibre tested ($S = L_0 \cdot \pi \cdot D$) and V its volume ($V = L_0 \cdot \pi \cdot D^2/4$). This assumes that the fibres are circular, which is the case for most of the commercial ceramic fibres as seen in Fig. 1.

The experimental failure probabilities $P_R = 1 - P_S$ are determined from the tensile tests in the following way. N_{L_0} fibres tested at the same gauge length L_0 are ranked in by increasing order of their failure stress. The probability of failure $P_R(i) = i/(N_{L_0}+1)$ is assigned to the ith fibre broken at $\sigma_{R,i}$ with $\sigma_{R,i-1} \leq \sigma_{R,i} \leq \sigma_{R,i+1}$.

The Weibull parameters m and θ can be determined using a least square fit linear regression of the plot $\ln[-\ln(1 - P_R(i)]$ as function of $\ln(\sigma_{R,i})$, since Equations 1 or 2 gives

$$\ln[-\ln(1 - P_R)] = m \cdot \ln(\sigma) + \ln\left(\left|\frac{V}{S}\right.\right) + \ln(\theta) \quad (3)$$

4. The fibre diameter is not constant

For the above method to be valid the fibre diameter has to be constant. Ceramic fibres are obtained from the simultaneous spinning of hundreds of precursor fibres followed by their pyrolysis. Small variations in the hole diameters of the spinneret induce diameter variations from one fibre to another in the same bundle of ceramic fibres. This spinning step requires precursor of sufficient viscosity, which can lead to significant diameter variations along the same precursor fibre. This has been encountered for some SiC based fibres. The conversion to ceramic fibres is accompanied by an important volume change, which may also induce a diameter variation. Differences up to 4 μm in the fibre diameter in a same bundle are not rare as seen in Fig. 2 [6].

The use of a mean diameter in the determination of the Weibull parameters produces a significant error [7, 8]. Larra-Curzio *et al*. [7] show that taking a mean diameter of 12 μm, the m value is underestimated by a factor 1.78 if the standard deviation is of 2 μm. The fibre diameter has to be known for each fibre tested. If the variation of the diameter along one fibre can be neglected, the diameter is measured prior to each tensile test. In the case of possible variation along the gauge length, the diameter should be measured at the location of the failure. In practice this is however not always feasible as the elastic energy released during the failure makes the fibre break into several pieces and the deposition of absorbing media on the fibre surface (paraffin, grease ...) is not without effect on the fibre tensile properties. In this case, the diameter profile along the gauge length is determined and the minimum diameter is taken into account. In the present study diameter variations along the 250 mm gauge lengths never exceeded 3% and were neglected, but individual fibre diameter was measured prior to each tensile test.

If the fibres present variations in their diameters from one fibre to another, an effective failure stress σ_E expressed as

$$\sigma_E = \sigma_R \cdot \left(\left|\frac{V}{S}\right.\right)^{1/m} \quad (4)$$

has to be introduced to reflect the effect of volume or surface variation on the failure probability. The ranking is then carried out on these effective failure stresses and the probability of failure $P_R(j) = j/(N_{L_0} + 1)$ is assigned to the jth fibre broken at $\sigma_{R,j}$ with $\sigma_{E,j-1} \leq \sigma_{E,j} \leq \sigma_{E,j+1}$. It can be seen that this ranking depends on the value of m which is sought. This value is estimated by an iterative calculation.

[1] Watson image shearing eye piece - M.E.L. Equipment Co.

[2] LSM 6000 - Mitutoyo.

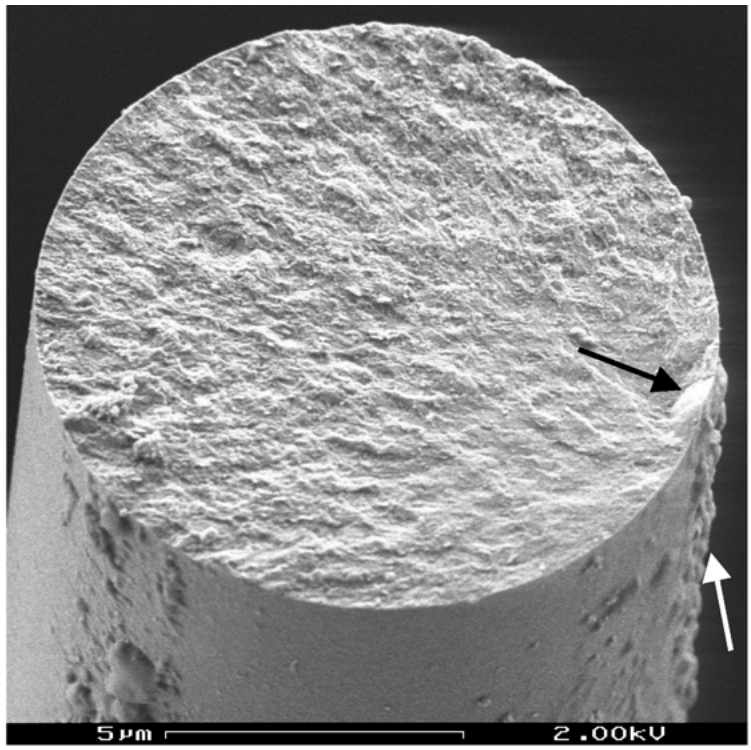

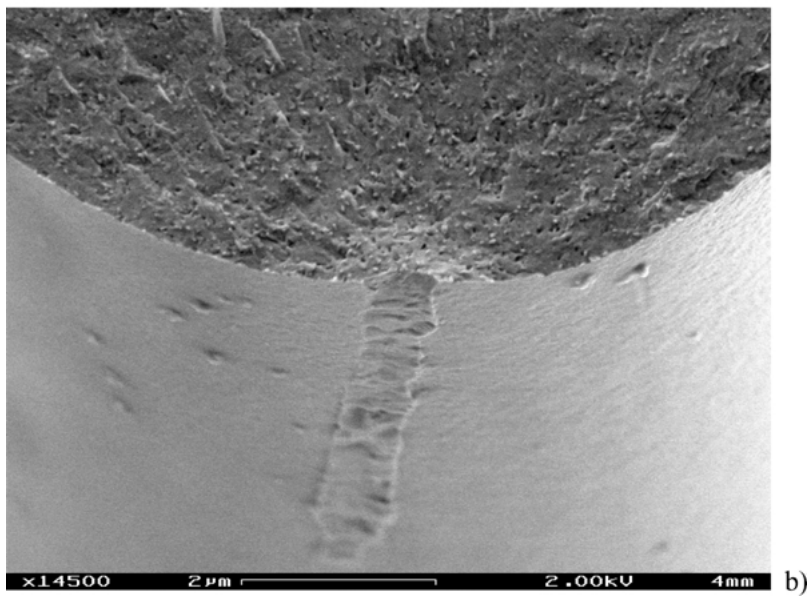

Figure 1 (a) Nextel 720 fibre: the fibre is circular in cross section. Failure is initiated from a surface defect (black arrow), associated to the line of contact with surrounding fibres (white arrow). (b) Detail of a welding line and associated critical defect.

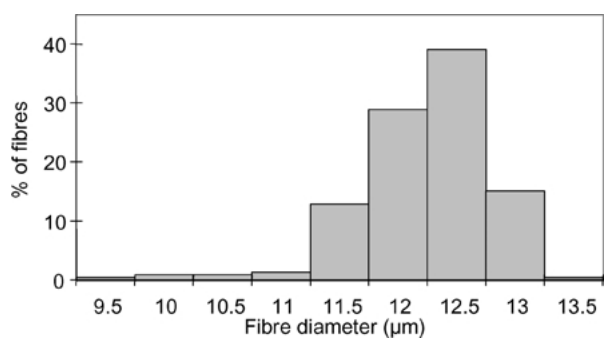

Figure 2 Diameter variation of Nextel 720 fibre. Diameters of 280 fibres (5 to 250 mm in length) were measured at different places, up to 6 for 250 mm lengths. The standard deviation along one fibre is 2.7%, but significant variations from one fibre to another were observed [6].

In the analysis of the Nextel 720 strength distribution 25 values of m, ranging from 2 to 8 by step of 0.25 were tested. For each m, the value of θ was determined to give the best fit between the experimental and the theoretical distributions of failure probability and among the 25 pairs (m, θ) determined by this analysis, the best fit was chosen. The appropriateness of the fit was estimated by a Kolmogorov-Smirnov criterion, which gives the probability P_{fit} that the experimental failure probability P_{exp} corresponds to the failure probability P_{W} predicted by a Weibull law as a function of λ.

$$\lambda = \text{Max}\,|P_{\text{W}}(\sigma_{\text{E,i}}) - P_{\text{exp}}(\sigma_{\text{E,i}})| \cdot \sqrt{N_{\text{L}_0}} \quad (5)$$

$$P_{\text{fit}}(\lambda) = 1 - \sum_{k=-\infty}^{\infty} (-1)^k e^{-2k^2\lambda^2} \quad (6)$$

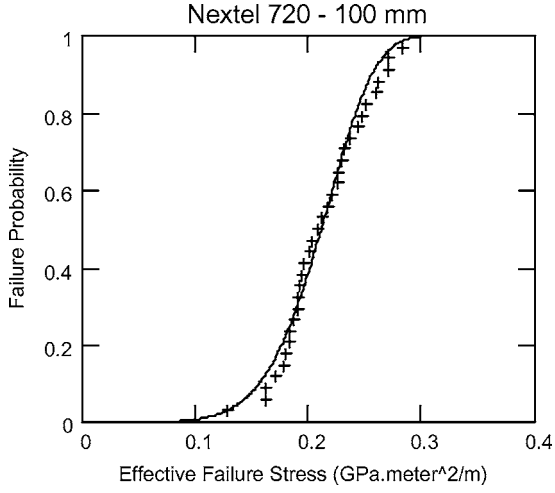

Figure 3 Distribution of the failure stress for 33 fibres with a gauge length of 100 mm. $m = 6.25, \theta = 1.15.10^4$ GPa$^{-6.25}$·m^{-2}, $P(\lambda) = 0.99$.

Fig. 3 shows the result of this iterative calculation for a gauge length of 100 mm. The best fit was found for $m = 6.25$ and $\theta = 1.15.10^4$ GPa$^{-6.25} \cdot$ m^{-2} with a Kolmogorov-Smirnov criterion of 0.99.

5. The estimation of *m* depends on the gauge length

The distribution of the 30 failure stresses obtained at 100 mm with the Nextel 720 fibre seems to be correctly fitted by an unimodal Weibull law ($P(\lambda)$ close to unity). It is common that publications describing the failure stress distributions of a ceramic fibre stop their investigation at this point [9–11] . From the experimental determination of m and θ at 100 mm, one should be able to predict the failure stress distribution for various gauge lengths. This has been checked by testing an average of thirty fibres in tension at 5 other gauge lengths L_0 ($L_0 = 5$, 10, 25, 50, 250 mm). The experimental stress distributions were however not correctly described with the Weibull parameters determined at 100 mm. A separate treatment of the results for each gauge length by the method described in paragraph 4 gave distinct m values ranging from 3.75 to 6.75 as shown in Fig. 4. This variation of m with the gauge length is not compatible with a Weibull law as written in Equations 1 or 2. Several hypotheses have been proposed to explain these discrepancies.

6. The selection of the fibre during sample preparation affects the strength distribution

The extraction of individual brittle ceramic fibres from a bundle is an arduous task. Weaker fibres can break during fibre preparation, so that a selection of the stronger fibres is unintentionally made which affects the strength distribution. As longer lengths of fibres are more difficult to extract than smaller ones, the bias introduced during specimen preparation is more important for longer gauge lengths. This fibre selection has been identified by some authors as a major shortcoming when testing single fibres [12]. The effect of this selection on the fibre distribution can be modelled in the following way:

Let us consider a fibre strength distribution in the bundle following a two-parameter Weibull law (m, θ), and make the assumption that the fibres having a strength lower than a threshold stress σ_{th} break during their extraction from the bundle or mounting on the cardboard frame. The survival probability of a fibre subjected to a tensile stress σ, taking into account that the fibre is first extracted from the bundle, becomes

$$P_S(\sigma_R \geq \sigma | \sigma_R \geq \sigma_{th}) = \frac{P_S(\sigma_R \geq \sigma)}{P_S(\sigma_R \geq \sigma_{th})} \quad (7)$$

$$= \exp\left[-\theta . \left|\frac{S}{V}\right| \cdot \left(\sigma^m - \sigma_{th}^m\right) \right] \quad (8)$$

It has to be noticed that this threshold stress induced by a selection of the fibres by the operator has not the same physical signification that the threshold stress σ_u usually found in the following expression of the survival probability: $P_S(\sigma_R \geq \sigma) = \exp(-\theta \ V \cdot (\sigma - \sigma_u)^m)$. In this later case σ_u is the value of the intrinsic stress below which $P_S = 1$ prior to any selection. In our case $\sigma_u = 0$.

Fig. 5 models the effect that a selection of fibres ($\sigma_{th} = 0.67$ GPa, $D = 12.5$ μm) would have on the strength distribution at $L_0 = 250$ mm. This would affect the concavity of the curve at the low stresses but could not explain the discrepancies in the m values observed.

7. The reliability of the *m* value relies on the number of fibres tested

An other hypothesis to explain this variation was that the 30 number of fibres tested at each gauge length was too low to allow a good reliability in the Weibull parameter determination [8, 13].

Simulations of thousands strength distributions were made, to determine the effect of the number of tested fibres on the reliability of the m determination. The following method was chosen for each simulation: 30 numbers between 0 and 1 were drawn randomly, so as to give a set of failure probabilities P_i, with $i = 1$ to 30. A failure stress σ_i as assigned to each P_i by the following relationship:

$$\sigma_i = \left[\frac{-\ln(1 - P_i)}{S \cdot \theta} \right]^{1/m} \quad (9)$$

with $m = 4$, $\theta = 7.22 \times 10^4$ GPa^{-4} m^{-2}, $S = (12.5 \times 10^{-6}) \cdot \pi \cdot (25 \times 10^{-3})$ m^2.

These 30 failure stresses simulated the result of a set of 30 tensile tests for 25 mm fibres of a constant diameter of 12.5 μm and with a defect distribution described by a Weibull law with the above m and θ parameters. The m^* and θ^* parameters were then newly estimated from these 30 simulated failure stresses using the method described in paragraph 4. The result of thousand simulations is presented in grey in Fig. 6. The mean m^* value was 3.96 and the standard deviation was 0.68.

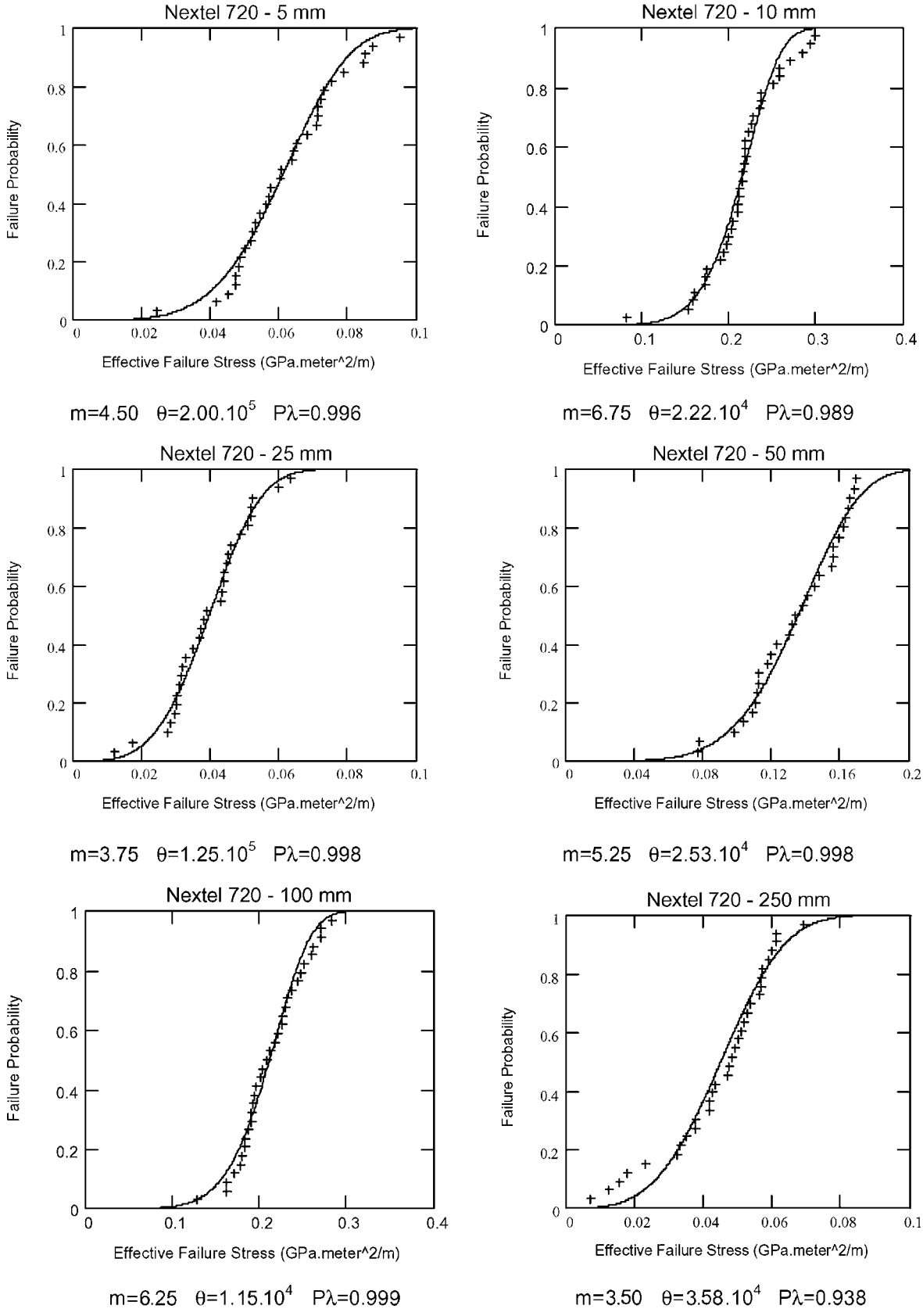

Figure 4 The separate analysis of the failure stress distribution at gauge lengths of 5, 10, 25, 50, 100, 250 mm gives distinct Weibull parameters.

The number of simulated tests was then extended to 180. The results of thousand simulations, shown in black in Fig. 6 were showing a lower dispersion than with 30 fibres with a mean value $m^* = 4.03$ and a standard deviation equal to 0.29.

The introduction of the effective failure stress $\sigma_E = \sigma_R \cdot (|_S^V)^{1/m}$ allowed the 180 experimental failure stresses obtained with the six gauge lengths to be analysed on the same curve. Fig. 7 shows that all the experimental data could be gathered in one single curve giving $m = 4$ and $\theta = 7.22.10^4$ GPa^{-4} m^{-2}.

It can be seen that the precision of the determination of m was significantly improved by the use of the effective stress allowing the 180 test results to be analysed on

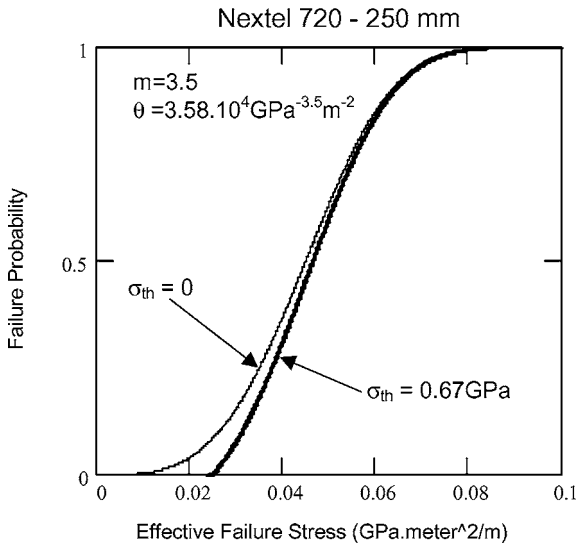

Figure 5 The effect of a fibre selection during specimen preparation on the strength distribution is modelled (bold curve) and compared to the strength distribution without fibre selection.

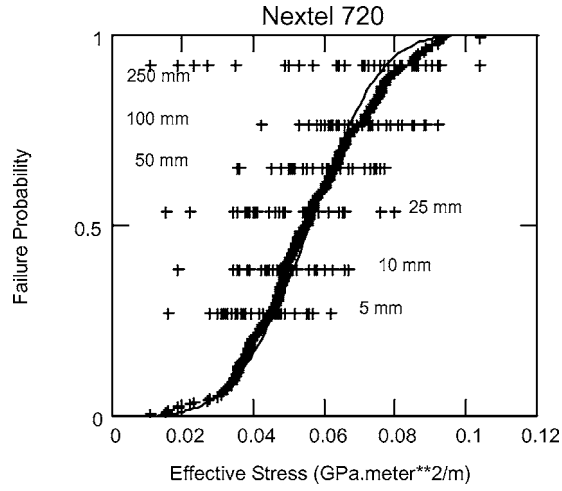

Figure 7 The 180 failure stresses obtained from the 30 tensile test results at 6 gauge lengths are analysed on the same curved by using an effective failure stress. $m = 4$, $\theta = 7.22 \times 10^4$ GPa^{-4} m^{-2}, $P(\lambda) = 0.42$. The horizontal lines correspond to the repartition of the effective failure stresses. Every point of the experimental failure probability curve is vertically aligned with a cross of one of the horizontal lines corresponding to the experimental gage length used for this point. For example the first and last points have been obtained at 250 mm.

the same distribution. In addition, the range of values of m^* obtained by simulations covered the range of values obtained from experiments. This is a confirmation of the validity of the model.

8. The flaw density fluctuates along the length

A closer examination of Fig. 7 reveals a deviation of the experimental results from the theoretical curves from a failure probability of 0.75, showing a saturation of the experimental probability. Moreover, longer gauge lengths give rise to higher effective failure stresses in average as shown by the gradual shift of the horizontal lines when going from 5 mm to 250 mm. This can also be shown by re-examining separately the results at each gauge length with the Weibull parameters obtained in paragraph 7. It can be seen from Fig. 8 that there is a progressive shift of the experimental stress distribution with respect to the theoretical curve.

The aim of the effective failure stress was to balance the volume effect in the failure stress. The $L_0^{1/m}$ variation of σ_E is derived from the expression of the failure probability in Equations 1 or 2. This formulation makes the assumption that the flaws follow a Poisson point process number in the length, so that the survival probability P_S ($P_S = 1 - P_R$) is a multiplicative function of the length

$$P_S(\sigma, L_1 + L_2) = P_S(\sigma, L_1) \cdot P_S(\sigma, L_2) \qquad (10)$$

It is however shown that the $L_0^{1/m}$ variation of σ_E does not allow a valid description of the length effect

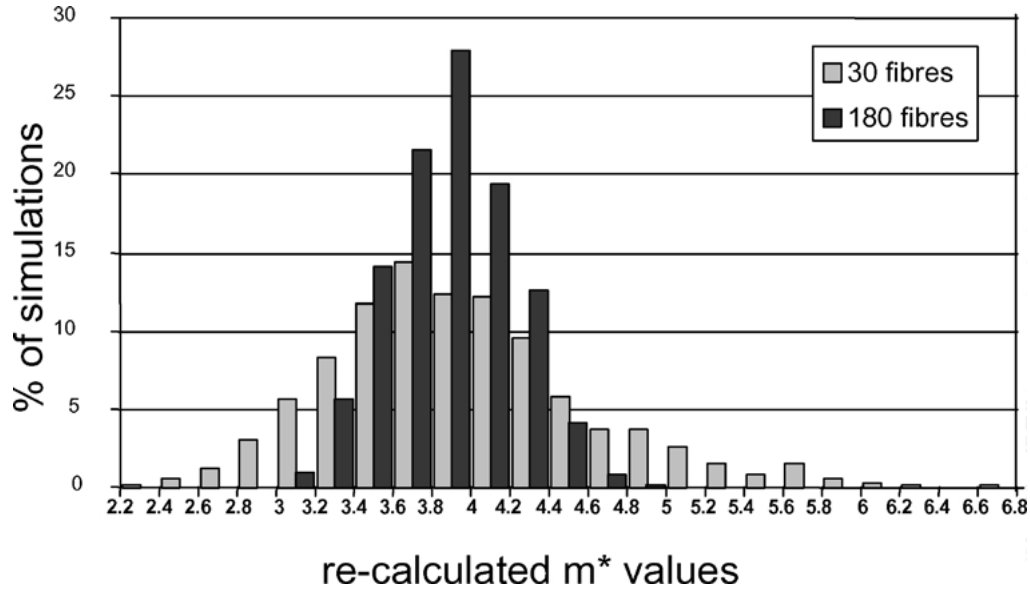

Figure 6 Frequency histogram of the recalculated m^* values from 1000 sets of 30 (grey) and 1000 sets 180 (black) failure stresses randomly drawn from a Weibull distribution with $m = 4$.

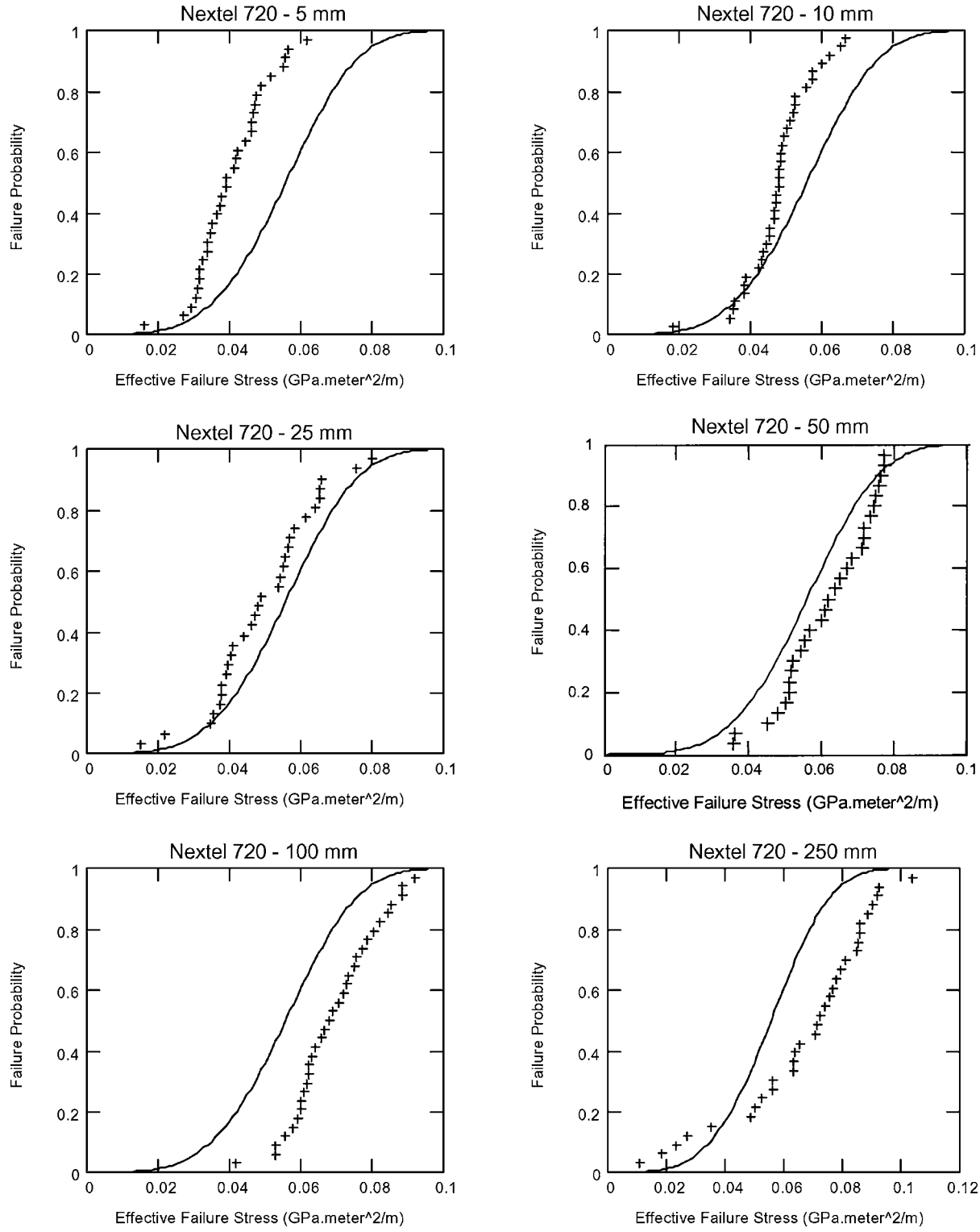

Figure 8 The Weibull parameters deduced in Fig. 5 by bringing together the 6 gauge length results do not allow the experimental failure probability at a given gauge length to be predicted. A progressive shift from the left to the right of the theoretical curve is observed when increasing the gauge length.

in the fibre failures. This means that there should be a fluctuation in the flaw density along the length or that the mean amount of flaws per unit length is a random variable, changing from one fibre to the other.

Similar strength data processing was carried out with tensile test results obtained with SiC based ceramic fibres [14], the NL200 and Hi-Nicalon fibres from Nippon Carbon and the Tyranno ZM and Tyranno Lox M from Ube Industries and with the Nextel 650 alumina-zirconia fiber from 3M [15]. The resulting curves are shown in Fig. 9. These curves exhibit the same trends as those found in Fig. 7, that is the deviation to the theoretical curve for the highest probability and the higher effective strengths at longer gauge lengths. This shows that the length dependence of the flaw density has to be considered for a wide range of ceramic fibres.

The fluctuation in the flaw density along the length can be expressed in the Weibull model by the introduction of a β exponent on the gauge length (as initially

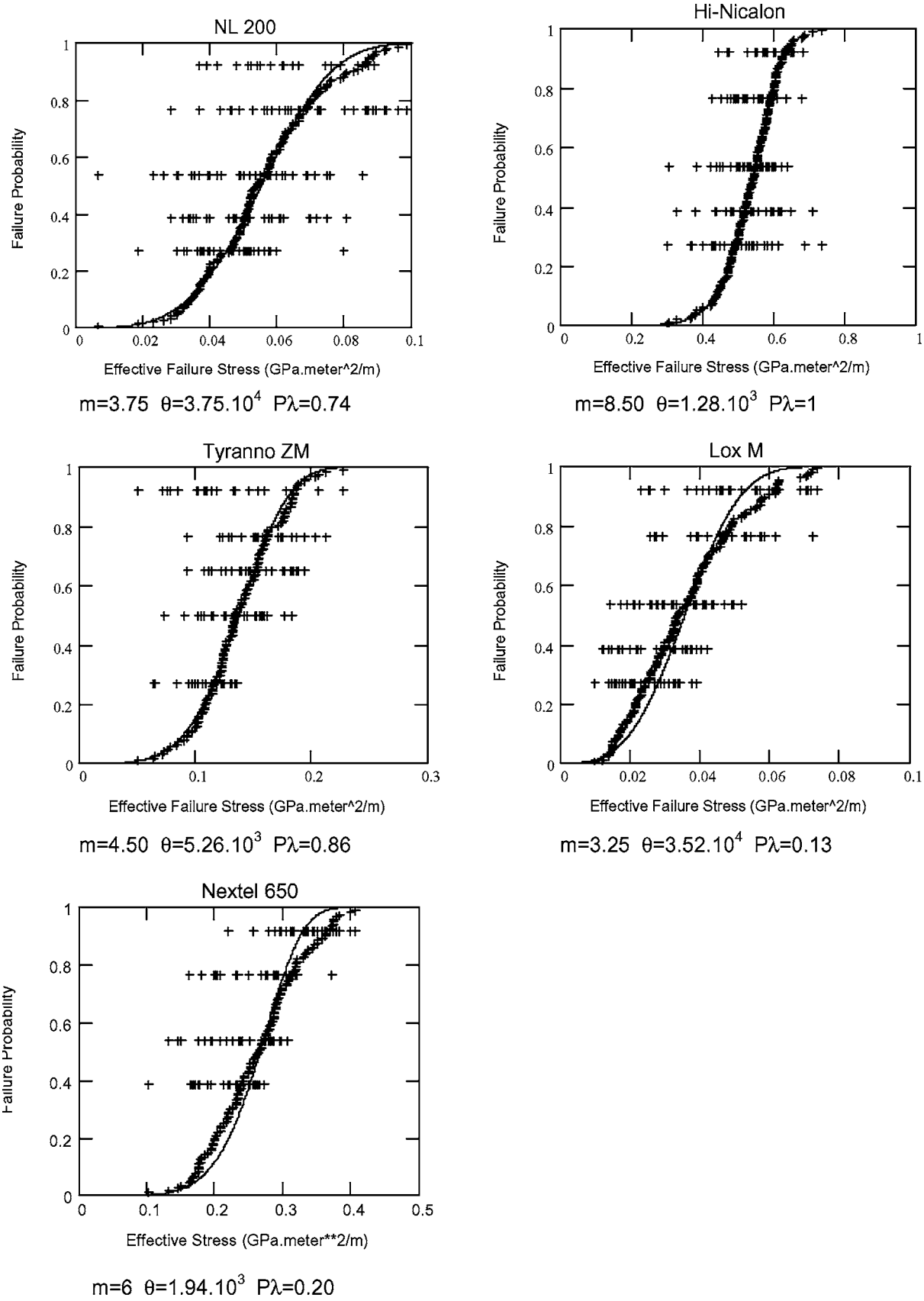

Figure 9 Failure stress distributions of four fine SiC based fibres, the NL200 and Hi-Nicalon fibres from Nippon Carbon and the Tyranno ZM and Tyranno Lox M from Ube Industries and Nextel 650 fibre from 3M . The methodology described in paragraph 7 has been applied to fit the experimental curves. A deviation to the theoretical curves for the highest probabilities and higher effective strengths at longer gauge lengths are noticed for the NL200, Tyranno Lox M, Tyranno ZM and Nextel 650.

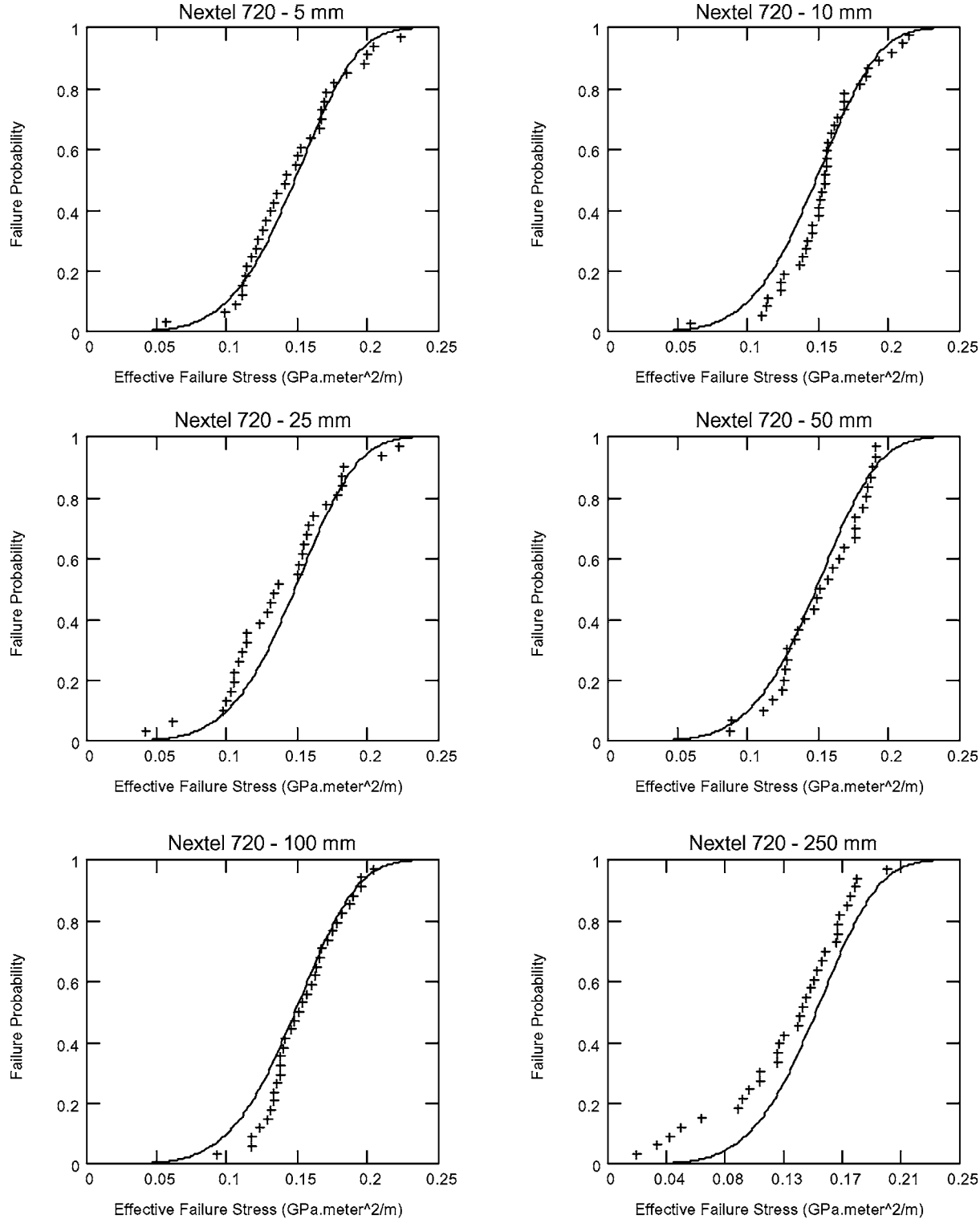

Figure 10 The prediction of the failure probability of Nextel 720 fibres for the six gauge lengths using the same Weibull parameters ($m = 4.8$, $\theta = 6.614\ \mathrm{GPa}^{-4.8} \cdot \mathrm{m}^{-1-\beta}$) can be obtained with a power law contribution of the gauge length ($\beta = 0.425$).

proposed by Watson and Smith [16] to account for a random distribution of the fibre diameters), when the density is a random variable with a stable distribution [17]:

$$P_S(\sigma_R \geq \sigma, L_0, D) = \exp\left[-\theta \cdot \sigma^m \cdot (L_0)^\beta \cdot \begin{vmatrix} \pi D \\ \pi D^2/4 \end{vmatrix} \right] \quad (11)$$

The estimation of the parameters m, θ and β was made in the following way: the strength distributions are considered separately for each gauge length, using as effective failure stress:

$$\sigma_E = \sigma_R \cdot (L_0)^{\beta/m} \left(\begin{vmatrix} \pi D \\ \pi D^2/4 \end{vmatrix} \right)^{1/m} \quad (12)$$

The three parameters giving in average the best fit for the six curves are looked for. For the Nextel 720 fibres the best fit was found for $m = 4.8$, $\theta = 6.61.10^3$ $\mathrm{GPa}^{-4.8}$ $\mathrm{m}^{-1-\beta}$ and $\beta = 0.42$, and the corresponding curves are shown in Fig. 10. If the six gauge lengths

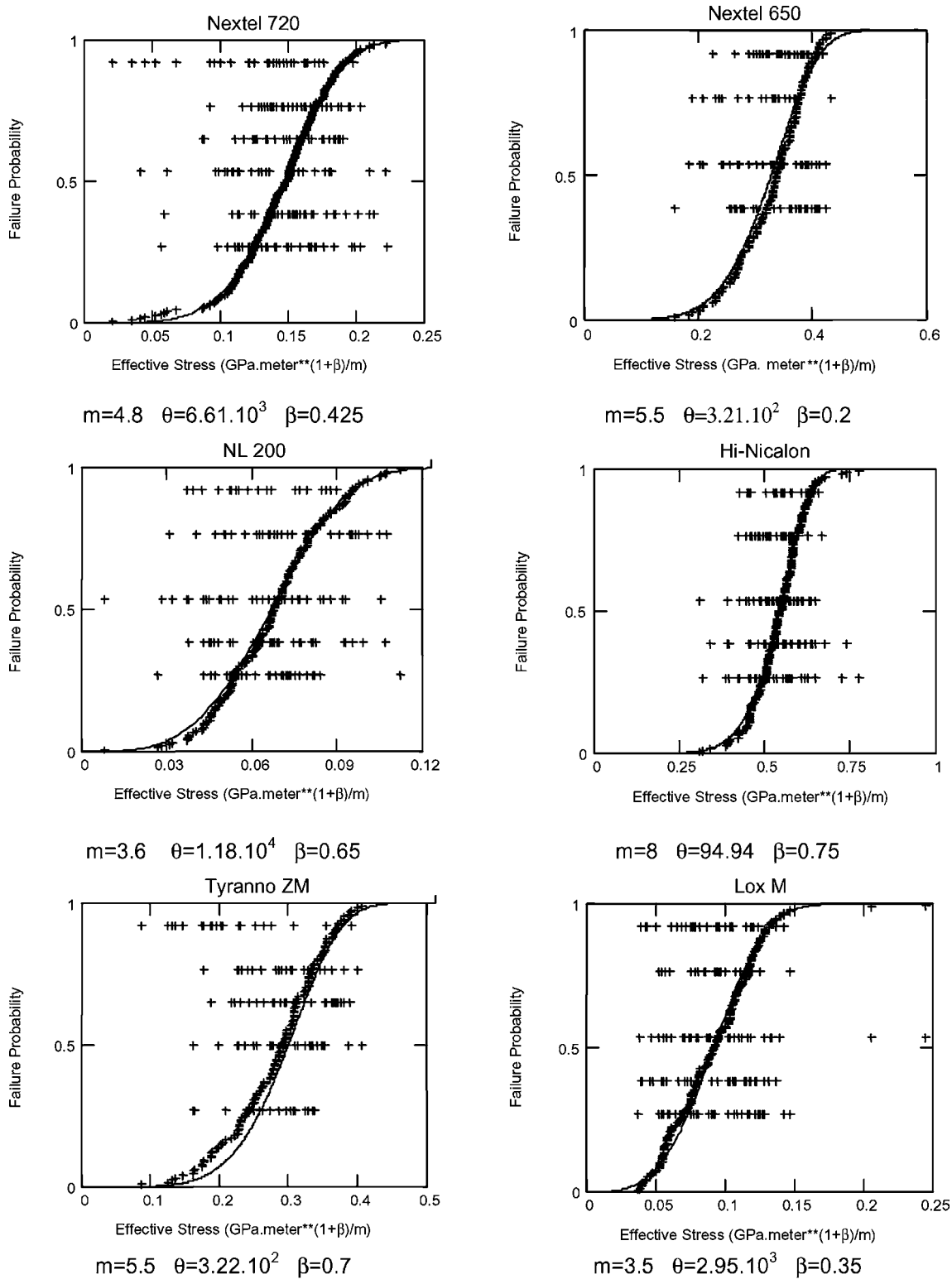

Figure 11 The same methodology was applied to fit experimental failure stress distributions obtained on 3M-Nextel 650 alumina-zirconia fibres and SiC based fibres.

are now plotted on the same curve, Fig. 11, it can be seen that the gauge length are well distributed among the effective failure stresses and that the theoretical and experimental curves fit well even for the highest failure probabilities.

9. Physical interpretation

From our experimental results, it is clear that a distribution function of the fracture stress with a gauge length effect which is non linear in L_0, gives a correct description of our data. In several papers, this is attributed to statistical fluctuations of the diameter of fibres: the diameter of each fibre is considered as a realisation of a random variable [16], or is changing in a random fashion along the fibre [18]. However the theoretical derivation of the non linear scale effect is unclear with these last assumptions. Let us consider a radius $R(x)$ changing along the fibre and make the assumption that θ, giving the intensity of defects, is constant along the

fibre. The stress applied on the section is then

$$\sigma(x) = \frac{F}{\pi \cdot R^2(x)} \tag{13}$$

where F is the applied load. The survival probability can then be written

$$P_S(\sigma_R \geq \sigma) = \exp\left(-\int_0^L 2\pi R(x) \cdot \theta \sigma^m(x)\, dx\right) \tag{14}$$

$$P_S(\sigma_R \geq \sigma) = \exp\left(-2 \cdot \pi^{1-m} \cdot \theta \cdot F^m \int_0^L R(x)^{1-2m} dx\right) \tag{15}$$

Let us introduce an effective radius R_{eff} so that R_{eff}^{1-2m} corresponds to the mean value of $R(x)^{1-2m}$ over the gauge length L:

$$\frac{1}{L}\int_0^L R(x)^{1-2m} dx = R_{eff}^{1-2m} \tag{16}$$

Then

$$P_S(\sigma_R \geq \sigma) = \exp\left(-2 \cdot \pi^{1-m} \cdot \theta \cdot F \cdot R_{eff}^{1-2m} \cdot L\right) \tag{17}$$

This demonstrates that a fluctuation of diameter along a fibre can only generate a linear effect in L ($\beta = 1$).

In [17] is introduced a fluctuating intensity (average number per unit length) of defects. When this intensity is considered for each fibre as a realization of a random variable with a stable distribution with coefficient $\beta < 1$ [19], the probability of non fracture is exactly given by Equation 11. Therefore, the interpretation of our results involves fluctuations of the density of defects on a large scale (much larger than the gauge length), according to probable fluctuations of the physical conditions during the elaboration of fibres. In the case of the Nextel oxide fibres, fracture morphology observation indicates that failure is initiated from discontinuous surface lines running parallel to the fibre axis. These lines, shown in Fig. 1, originate from contacts with neighbouring fibres in the bundle inducing their welding during sintering [11]. Failure distribution is then related to the interfilament distance distribution during processing, which can fluctuate at a large scale. In addition along these weld lines one can expect a much higher intensity of defects, as compared to healthy fibres. This is in agreement with our assumption of interfibre fluctuation of intensity of defects. The polymer derived silicon carbide based fibres studied exhibit higher value of β than Nextel 720 fibres, i.e., less fluctuation of the defect density, except for Tyranno Lox-M fibres. Fracture in these fibres is mainly caused by surface notches due to mechanical abrasion during the process. Unfortunately, information about process details is not available in the literature to go further in the interpretation.

10. Conclusions

From the analysis of a large data set on the tensile strength of the mullite alumina Nextel 720 fibre, we could demonstrate the following points:

– For every gauge length, the statistical distribution of strengths follows the Weibull weakest link model, according to defects located in the surface of fibres.

– The size effects expected from the standard Weibull model is not appropriate.

– A power law size gauge length effect could correctly describe the data. It corresponds to a particular (stable) distribution of the random intensity of defects, as a result of large-scale fluctuations of defects.

– This methodology can be applied to other types of ceramic fibres.

– Fluctuation in the fabrication process of the fibres can be revealed by the knowledge of the coefficient β of the stable distribution.

Acknowledgements

This study is based on experimental results collected by N. Hochet, F. Deléglise and A Quintin-Poulon for their PhD works achieved in the research group of AR Bunsell. The authors are indebted to them. This study was sponsored by a DGA-DRET convention (92 017 00 012) and EURAM-BRITE programs (BRPR-CT-95-0110, BRPR-CT97-0609).

References

1. S. L. PHOENIX, *Fibre Sci. Tech.* **7**(1) (1974) 15.
2. T. S. CREASY, *Compos. Sci. Tech.* **60** (2000) 825.
3. F. DELÉGLISE, M. H. BERGER, D. JEULIN and A. R. BUNSELL, *J. Eur. Ceram. Soc.* **21** (2001) 569.
4. D. M. WILSON, S. L. LIEDER and D. C. LUENBURG, *Ceram. Eng. Sci. Proc.* **16**(5) (1995) 1005.
5. A. R. BUNSELL and P. SCHWARTZ, in "Comprehensive Composite Materials" Vol. 5 "Test Methods, Nondestructive Evaluation and Smart Materials," edited by L. A. CARLSSON, R. L. CRANE, K. UCHINO, A. KELLY and C. H. ZWEBEN (Elsevier, Amsterdam, 2000) p. 44.
6. F. DELÉGLISE, PhD thesis Ecole des Mines de Paris, France, 5th July 2000.
7. E. LARRA-CURZIO and C. M. RUSS, *Ceram. Eng. Sci. Proc.* **20**(3) (1999) 471.
8. T. A. PARTHASARATHY, *J. Amer. Ceram. Soc.* **84**(3) (2001) 588.
9. C. MILZ, J. GOERING and H. SCHNEIDER, *Ceram. Eng. Sci. Proc.* **20**(3) (1999) 191.
10. J. LIPOWITZ, J. A. RABE, A. ZANGVIL and Y. XU, *ibid.* **18**(3) (1997) 147.
11. D. M. WILSON and L. R. VISSER, *Compos.* A **32** (2001) 1143.
12. Z. CHI, T.-W. CHOU and G. SHEN, *J. Mater. Sci.* **19** (1984) 3319.
13. C. BERDIN, G. CAILLETAUD and D. JEULIN, in Proceedings of the ICASP 7 Conference, edited by M. Lemaire, J.L. Favre and A. Mebarki, Paris, France, July 1995 p. 131.
14. N. HOCHET, PhD thesis, Ecole des Mines de Paris, France, 26th September 1996.
15. A. POULON-QUINTIN, PhD thesis Ecole des Mines de Paris, France, 26th April 2002.
16. A. S. WATSON and R. L. SMITH, *J. Mater. Sci.* **20** (1985) 3260.
17. D. JEULIN, *Annales des Composites* **1** (1996) 23.
18. Y. ZHANG, X.WANG, N. PAN and R. POSTLE, *J. Mater. Sci.* **37** (2002) 1401.
19. W. FELLER, in "An introduction to Probability Theory and its Applications," Vol. 2 (J. Wiley, New York, 1971).

Received 11 July 2002
and accepted 21 March 2003